Hybrid force/position control of robotic arms manipulating in uncertain environment based on adaptive fuzzy sliding mode control

Abbas Karamali Ravandi[a], Esmaeel Khanmirza[a,*], Kamran Daneshjou[a]

[a]*School of Mechanical Engineering, Iran University of Science and Technology, Narmak, Tehran, Iran*

Abstract

In this study, the hybrid force/position control of robotic manipulators operating in uncertain environments is addressed by integrating the fuzzy logic with conventional sliding mode control (SMC). After decomposition of the manipulator dynamics into position, force, and redundant joint subspaces, the universal approximation capability of fuzzy systems is employed to approximate the equivalent part of the control input constructed based on SMC concept. The robust part of the controller is estimated by an adaptive PI controller to compensate for deviations due to the presence of model uncertainties and perturbations. Furthermore, some adaptation laws are derived to update the parameters online when some changes in the system dynamics are made. The proposed adaptive fuzzy sliding mode control (AFSMC) requires the minimum information about the manipulator dynamic structure and environment physical properties among the other hybrid force/position control methods presented so far. Indeed, it needs neither estimation of the dynamic model nor bounds of uncertainties in advance. The asymptotic stability of the proposed controller is also proved in the sense of Lyapunov theorem. The simulation results show the good performance of the proposed controller in coping with uncertainties. The proposed scheme is also compared with standard SMC methodology, and its superior robustness is shown in comparison with those methods which require an estimation of the plant mathematical model.

Keywords: Manipulator, Hybrid force/position control, Fuzzy sliding mode control, Adaptive control

*Corresponding author
Email address: khanmirza@iust.ac.ir (Esmaeel Khanmirza)

1. Introduction

In various industrial applications, there are many situations where robotic manipulator come in long-time contact with the environment. The tasks such as grinding, welding, and deburring represent some examples of applications where the end-effector of the manipulator performs operations on a surface. The successful execution of such tasks is guaranteed by simultaneous and accurate control of motion and interaction forces developed during contact. On the other hand, the dynamic structure of industrial manipulators is often difficult to be identified and modeled. This problem also exists to determine the physical properties of the contacted environment. Therefore, on the one side, synthesizing a precise model-dependent controller is a challenging problem and on the other side, designing the control laws based on the simplified version of the dynamics may lead to its failure in real applications.

In the literature, manipulators force-control schemes are often categorized into direct and indirect methods [1]. Indirect force control methods describe the interaction model of the robot and environment with an equivalent mass-spring-damper. Then, the force control is achieved through position control of the end-effector by adjusting the equivalent system parameters [2]. Direct methods, instead, try to regulate the desired force trajectory at the robot tip by the closure of the force measurement in a control loop. The hybrid force/position control which is a subset of direct methods is applied when the force is supposed to be controlled along certain constrained directions whereas the motion of the end-effector to be controlled in unconstrained directions [2].

In many actual situations, the manipulators operate in and contact with unidentified environments. In addition, the manipulators are often structurally complex and their accurate dynamic model identification is cumbersome. Therefore, it is mandatory to use the methods for manipulator force-control with robustness against uncertainties and parameters variation. SMC and adaptive control schemes are two well-known representatives of robust control methods that have their own unique merits [3–6]. Yu et al. [3] presented a combination of adaptive fuzzy controller and reduced-order observer for position tracking of the chaotic permanent synchronous motor. Fuzzy logic systems (FLSs) and observer are used to approximate unknown functions and to calculate angular speed, respectively. By the proposed method, the requirement for measuring the speed signal of motors is removed and the number of adaptive parameters is reduced. A neural adaptive

2

robust control strategy for output tracking control of a class of multi-input multi-output (MIMO) uncertain systems was proposed by Lian et al. [4]. In this study, a network of novel variable-structure radial basis function (RBF) is introduced as an approximator of unknown system dynamics. Under the effects of input dead-zone and predefined performance, a new adaptive fuzzy controller was reported by Wang et al. [5] to guarantee the tracking performance of the networked industrial processes. The FLS is used to approximate the unknown nonlinear function. Shi [6] synthesized an SMC scheme for a class of fractional-order nonlinear systems using a fractional-order sliding mode disturbance observer in the presence of external unknown disturbances.

For motion and force control of manipulators in particular, Kwan [7] presented a sliding adaptive controller with robustness to parameters variation in both manipulator and motor dynamics. Hybrid force/position control of manipulators with flexible joints using adaptive sliding mode control (ASMC) concept was studied by Farooq et al. [8]. Considering uncertainties about the kinematics and dynamics of the manipulators, an ASMC Jacobian motion and force control was investigated by Cheah et al. [9]. A robust adaptive hybrid force/position control of two manipulators was proposed by Mohajerpoor et al. [10] for handling an unknown object and interacting with the environment, cooperatively. The internal wrenches developed between the objects and robots are controlled, independently.

The design basis of adaptive and SMC methods relies on the mathematical model of the system. When the system dynamics is getting more complicated, handling the system by the conventional model-dependent control methods becomes more difficult. Moreover, in order to design the control laws for SMC in particular, the bounds of uncertainties and disturbances should be determined. This dependency on the dynamic equations and bounds of uncertainties and disturbances might weaken the system performance, noticeably.

Fuzzy systems (FS) and neural networks (NNs) are employed as two effective tools to approximate the nonlinear smooth functions. Combining adaptive control and/or SMC methods with FS or NN has led to outstanding results in robustness against structured and unstructured uncertainties, parameters variation, and external disturbances [11–17]. Fei and Cheng [11] proposed a novel three-layer recurrent neural network (RNN) to approximate unknown dynamics. An adaptive dynamic global sliding mode controller which is constructed based on PID sliding surface is combined with an RBF neural estimator to control a three-phase active filter by Chu et al. [12]. The RBF estimator is used for chattering elimination. A new fractional-order sliding mode controller was proposed by Fei and Lu [13] in which a fractional order term is included in the sliding surface. The requirement

3

for determining the bounds of uncertainties are also relaxed using an RBFNN.

Chen et al. [14] proposed an AFSMC architecture by which the unknown time-varying actuator faults are compensated. The unknown nonlinearity is also approximated by an adaptive FLS. Zhang et al. [15] presented an ASMC for fuzzy systems with mismatched uncertainties and exogenous disturbances. A linear matrix inequality (LMI) condition for which the sliding surface exists is presented. The resultant sliding surface guarantees the asymptotic stability of the system. For controlling unknown chaotic systems, a robust adaptive fuzzy controller was presented by Poursamad and Davaie-Markazi [16]. The same authors extended this method to unknown chaotic MIMO systems. Some industrial applications of fuzzy control systems, especially those related to adaptive fuzzy ones, can be found in [18]. These robust intelligent-based combined methods were used successfully for induction servomotor systems [19, 20], four-bar linkage mechanism [21], anti-lock braking systems [22], trajectory tracking of robotic manipulators [23, 24], active suspension vehicle system [25], and quadrotor tracking control [26].

In order to hybrid force/position control of manipulators, Kumar et al. [27] developed an NN-based adaptive control in which the parametric uncertainties are learned using NNs. Lin et al. [28] investigated the hybrid position/force control of manipulators mounted on oscillatory base by applying an adaptive neuro-fuzzy inference system (ANFIS) based control scheme. Hsu and Fu [29] designed a hybrid adaptive fuzzy controller to solve the overwhelming complexity of the deburring process and imprecise knowledge about manipulators problems. Himanshu et al. [30] proposed an ANFIS-PD+I hybrid force/position controller with effective results in working on unspecified robotic manipulator dynamics in the presence of external disturbances. Kiguchi et al. [31] designed a fuzzy NN controller enabling the system to work with noisy force sensor signals and unknown vibrations caused by the tool, efficiently. An indirect adaptive fuzzy control method was designed for control of force and motion of industrial robots by Mendes and Neto [32].

The existing works on hybrid force/position control of manipulators rely on complete or partial knowledge of the system dynamics. Some of the papers develop the controllers based on the linear-in-parameter property of systems [7–9, 33, 34]. These control algorithms use the structure of the dynamics and factorize the mathematical model into a matrix called regression and a vector of some parameters which is unknown. Uncertainties are not included in the model regression matrix which indicates the high sensitivity of these control algorithms on the accuracy of dynamic modeling. The other relevant studies, whose controllers are based on ASMC concept, use an estimation of the dynamic model and bounds for uncer-

4

tainties [27–32, 35–37]. When the dynamic modeling becomes more complex and complete parameters identification is difficult or impossible, these control methods undermine the system performance. In addition, when the bounds of uncertainties are not known, the designer has to estimate them for designing the model-based controllers. When it comes to overestimating, the large control inputs might be needed and the input saturation limits might be violated. On the contrary, under-estimating the uncertainties causes the system failure in real situations where they go beyond the assumed bounds.

The motivating context of this paper originates from aforementioned chal-lenges. The main contribution of this paper is developing a robust intelligent-based controller for hybrid force/position control of robotic manipulators which is completely independent of dynamic modeling of the system and determining the bounds of uncertainties a priori. To this end, the dynamic model of the robotic manipulator performing operations on a surface is decomposed into force, posi-tion, and redundant joint subspaces. For controller design, the equivalent and robust parts of SMC method are approximated by Takagi-Sugeno-Kang (TSK) fuzzy system and an adaptive PI controller, respectively. The robust part is added to compensate for deviations of the estimated controller from the ideal one. Then, the parameters of the controller are adjusted online based on some adaptation rules extracted from the second stability theorem of Lyapunov. The first advantage of the presented method in the current paper compared with those mentioned earlier is that it is fully model-free and needs minimum information about the mechani-cal and geometrical properties of the robot and environment. In addition, unlike aforementioned papers, the requirement for determining uncertainty bounds is eliminated by this method and it is estimated using the proposed strategy. Besides, despite the high performance of the proposed method, it is structurally simple and easy to implement.

The rest of this paper is organized as follows: Section 2 describes the math-ematical modeling of the manipulators with rigid links and decomposition of the robot dynamics. Section 3 is devoted to synthesis procedure of a classical SMC and proposed AFSMC algorithm. The simulation results of the proposed method applied to a 2-link manipulator are given in section 4 and section 5 concludes the paper.

5

2. Mathematical Description of Rigid Manipulators

2.1. Robot Dynamic Equations

Consider an n-rigid link fixed-base manipulator performing some tasks on a rigid environment. The dynamic equations of motion are given by:

$$M(q)\ddot{q} + C(q,\dot{q})\dot{q} + G(q) = \tau - J^T(q)\overline{F} \tag{1}$$

where $q \in R^n$ is the vector of joint displacement, $M(q) \in R^{n \times n}$ is a positive definite symmetric matrix which denotes the inertia matrix of the robot, $C(q,\dot{q}) \in R^{n \times n}$ is the Coriolis matrix and consists of the terms related to centripetal forces, $G(q) \in R^n$ is a vector and contains the terms corresponding to the gravity effects. $\tau \in R^n$ represents the vector of input torques applied to the joints, $\overline{F} \in R^m$ is the interaction force between the end-effector and environment, and $J \in R^{m \times n}$ is the Jacobian matrix which relates the velocities of the joint and task spaces as follows:

$$\dot{x} = J(q)\dot{q} \tag{2}$$

where $x \in R^m$ is the vector of position and orientation of the end-effector (pose vector). The environment can be modeled as a frictionless and deformable plane. Therefore, the force $\overline{F}$ is related to the deformation of the environment, proportionally:

$$\overline{F} = \overline{K}(x - x_e) \tag{3}$$

where $\overline{K} \in R^{m \times m}$ is the environment stiffness matrix and x_e denotes the point on the environment at rest. In this study, the purpose is to control the force and position of the robot in two orthogonal directions. Therefore, it is useful to decompose the stiffness matrix as [38]:

$$\overline{F} = \left[\begin{array}{c} F \\ F' \end{array} \right] = \left[\begin{array}{c} K \\ K' \end{array} \right](x - x_e) \tag{4}$$

where $F \in R^l$, $F' \in R^{m-l}$, $K \in R^{l \times m}$, and $K' \in R^{(m-l) \times m}$. l represents the dimensionality of the force control subspace. There is also a useful property in the robot dynamics implying that $\dot{M}(q) - 2C(q,\dot{q})$ is skew-symmetric [1] which will be used later.

6

2.2. Robot Dynamics Decomposition

The aim of this section is to decompose the manipulator dynamics into three orthogonal subspaces, i.e. force, position, and redundant joint subspaces [38]. Before proceeding, the following identities are introduced:

$$I = J^+ J + J^-, \ I = K^+ K + K^- \tag{5}$$

where

$$
\begin{aligned}
J^+ &= J^T \left[J J^T \right]^{-1} \\
K^+ &= K^T \left[K K^T \right]^{-1} \\
J^- &= I - J^T \left[J J^T \right]^{-1} J \\
K^- &= I - K^T \left[K K^T \right]^{-1} K
\end{aligned}
\tag{6}
$$

where J^+ and K^+ denotes Moore-Penrose pseudoinverse and J^- and K^- are the projectors onto the null-spaces of J and K, respectively. According to the above identities, the joint velocity vector, $\dot{q}$, and the task space velocity vector, $\dot{x}$, can be decomposed as follows:

$$\dot{q} = J^+ J \dot{q} + J^- \dot{q} = J^+ \dot{x} + J^- \dot{q} \tag{7}$$

$$\dot{x} = K^+ K \dot{x} + K^- \dot{x} = K^+ \dot{F} + K^- \dot{x} \tag{8}$$

The second derivative of the pose vector of the end-effector by use of Eq. (2) is:

$$\ddot{x} = J \ddot{q} + \dot{J} \dot{q} \tag{9}$$

Using this relation and second derivative of the vector of joint displacement of the manipulator, Eq. (7), one may obtain:

$$\ddot{q} = J^+ J \ddot{q} + J^- \ddot{q} = J^+ \left(\ddot{x} - \dot{J} \dot{q} \right) + J^- \ddot{q} \tag{10}$$

On the other hand, taking derivative of Eq. (8) gives:

$$\ddot{x} = K^+ K \ddot{x} + K^- \ddot{x} = K^+ \ddot{F} + K^- \ddot{x} \tag{11}$$

Using the decomposed vectors of joint and task spaces, the decomposed dynamic equations of motion are obtained:

$$
\begin{aligned}
M \left(J^+ \left[K^+ \ddot{F} + K^- \ddot{x} - \dot{J} \dot{q} \right] + J^- \ddot{q} \right) & \\
+ C \left(J^+ \left[K^+ \dot{F} + K^- \dot{x} \right] + J^- \dot{q} \right) + G &= \tau - J^T \overline{F}
\end{aligned}
\tag{12}
$$

This equation is another representation of Eq. (1) in which the components of F, x, and q are decomposed into three orthogonal subspaces to facilitate the controller design.

7

3. Controller Design

3.1. Sliding Mode Control Design

First, the following sliding surface and tracking error are defined:

$$s_\eta = \left(\frac{d}{dt} + \lambda\right)^2 \int_0^t \tilde{\eta} d\tau, \ \eta = F, x, q$$

$$\tilde{\eta} = \eta - \eta_d \tag{13}$$

where λ is a positive constant and subscript d represents the desired values of variables. Also, the reference velocities are defined as:

$$\dot{q}_r = \dot{q} - s \tag{14}$$

Following the decomposition discussion presented in previous section, the sliding surface can be rewritten as:

$$s = \dot{\tilde{q}}_r = \dot{q} - \dot{q}_r = J^+ \dot{x} + J^- \dot{q} - \dot{q}_r$$
$$= J^+ \left(K^+ \dot{F} + K^- \dot{x}\right) + J^- \dot{q} - \dot{q}_r \tag{15}$$

After some algebraic manipulation, the following sliding surface is obtained:

$$s = J^+ \left[K^+ s_F + K^- s_x\right] + J^- s_q \tag{16}$$

where

$$s_F = \dot{F} - \dot{F}_r, \ s_x = \dot{x} - \dot{x}_r, \ s_q = \dot{q} - \dot{q}_r \tag{17}$$

$\dot{F}_r$ and $\dot{x}_r$ are defined similar to $\dot{q}_r$ in Eq. (14). Taking the first time drivative of Eq. (16) yields:

$$\dot{s} = \frac{dJ^+}{dt} \left[K^+ \left(\dot{F} - \dot{F}_r\right) + K^- \left(\dot{x} - \dot{x}_r\right)\right] + \frac{dJ^-}{dt} \dot{\tilde{q}}_r$$
$$+ J^+ \left[K^+ \left(\ddot{F} - \ddot{F}_r\right) + K^- \left(\ddot{x} - \ddot{x}_r\right)\right] + J^- \ddot{\tilde{q}}_r \tag{18}$$

Employing Eqs. (16) and (18), the manipulator dynamics can be rewritten as:

$$M\dot{s} + Cs = \tau - \tau_e - z \tag{19}$$

8

where

$$\tau_e = J^T \overline{F}$$

$$z = M \left[J^+ \left(K^+ \ddot{F}_r + K^- \ddot{x}_r - \dot{J}\dot{q} \right) - Q \right]$$

$$+ C \left[J^+ \left(K^+ \dot{F}_r + K^- \dot{x}_r \right) + J^- \dot{q}_r \right] + G$$

$$Q = \frac{dJ^+}{dt} \left[K^+ \left(\dot{F} - \dot{F}_r \right) + K^- \left(\dot{x} - \dot{x}_r \right) \right] + \frac{dJ^-}{dt} \check{q}_r \qquad (20)$$

The sliding mode-based controller is designed as follows:

$$\tau = - \left(\tau^{eq} + \tau^{rb} \right), \ \tau^{eq} = - \left(\tau_e + z \right) \qquad (21)$$

where τ^{eq} and τ^{rb} denote the equivalent and robust parts of the control input, respectively. If the plant model is exact and known completely, the following ideal controller, τ^{id}, stabilizes the system, asymptotically:

$$\tau^{id} = -\tau^{eq} - K_D s = - \left(\tau^{eq} + K_D s \right) \qquad (22)$$

To prove this, consider the following Lyapunov candidate function:

$$L = \frac{1}{2} s^T M s \qquad (23)$$

Differentiating the above equation with respect to time gives:

$$\dot{L} = s^T M \dot{s} + \frac{1}{2} s^T \dot{M} s = s^T \left(M \dot{s} + \frac{1}{2} \dot{M} s \right)$$

$$= s^T \left(M \dot{s} + C s \right) = s^T \left(-\tau^{eq} - K_D s + \tau^{eq} \right)$$

$$= - s^T K_D s < 0. \qquad (24)$$

in which the skew-symmetric property of $\dot{M} - 2C$ has been used. However, in practice, the system parameters are not certainly known and on the other hand, the system dynamics structure is not exact. The purpose of SMC concept is to make the error trajectories converge to the sliding surfaces and remain on them despite the presence of structured and unstructured uncertainties. Consider the following control law:

$$\tau = \tau_e + \hat{z} - K_D s - K_p \operatorname{sign}(s) \qquad (25)$$

where $\hat{z}$ is an estimation of z defined in (20). Substituting Eq. (25) into Eq. (19) yields:

$$M \dot{s} + C s = \Delta z - K_D s - K_p \operatorname{sign}(s) \qquad (26)$$

9

where $\Delta z = \hat{z} - z$, and K_p should be selected appropriately. Again, consider the Lyapunov candidate function introduced in Eq. (23) and differentiate it with respect to time:

$$
\begin{aligned}
\dot{L} &= s^T M \dot{s} + \frac{1}{2} s^T \dot{M} s = s^T \left(M \dot{s} + \frac{1}{2} \dot{M} s \right) \\
&= s^T \left(\Delta z - K_D s - K_p \operatorname{sign}(s) \right) \\
&= \sum_{j=1}^{n} s_j \left[\Delta z_j - K_{pj} \operatorname{sign}\left(s_j \right) \right] - s^T K_D s \\
&= \sum_{j=1}^{n} \left[s_j \Delta z_j - K_{pj} |s_j| \right] - s^T K_D s \\
&\leq \sum_{j=1}^{n} \left[|s_j| |\Delta z_j| - K_{pj} |s_j| \right] - s^T K_D s \\
&= \sum_{j=1}^{n} |s_j| \left[|\Delta z_j| - K_{pj} \right] - s^T K_D s
\end{aligned}
\tag{27}
$$

If $K_{pj} \geq |\Delta z_j|$, it can be conclude that $\dot{L} < 0$ for $s_j \neq 0$.

3.2. Adaptive Fuzzy Sliding Mode Control Design

Although the robustness against uncertainties is ensured by appropriate tuning of the design parameters, the SMC scheme performance is degraded by deviation of the estimated plant model structure from the exact one. In other words, the less the controller relies on the mathematical model, the more it is reliable against uncertainties. This section provides the mathematical description of the proposed intelligent-based controller which is completely model-free and robust against uncertainties.

By resorting to the universal approximation capability of the fuzzy systems, τ^{eq} can be approximated as follows. Considering TSK fuzzy system and s_j as the input and τ_j^{fuzz} as the output, the fuzzy if-then rules for the j'th link of the manipulator is defined as:

Rule r: If s_j is A_j^r then $\tau_j^{fuzz} = \theta_j^r$, $r = 1, \cdots, n_r$

where θ_r^j is the fuzzy singleton of the output of the r'th rule and A_j^r is a fuzzy

10

set with the following Gaussian membership function (MF):

$$\mu_{A_j^r}\left(s_j\right) = \exp\left[-\left(\frac{s_j - c_j^r}{\sigma_j^r}\right)^2\right] \tag{28}$$

where c_j^r and σ_j^r are the center and variance of the MFs. By using singleton fuzzifier, product inference, and center average defuzzifier, the following relation holds for the output of the j'th link of the robotic arm:

$$\tau_j^{fuzz}\left(s_j\right) = \frac{\sum_{r=1}^{n_r} \theta_j^r \mu_{A_j^r}\left(s_j\right)}{\sum_{r=1}^{n_r} \mu_{A_j^r}\left(s_j\right)} \tag{29}$$

The above relation can be rewritten as:

$$\tau_j^{fuzz}\left(s_j \mid \theta_j\right) = \theta_j^T W_j \tag{30}$$

in which

$$\theta_j = \left[\theta_j^1, \cdots, \theta_j^{n_r}\right]^T, \ W_j = \left[W_j^1, \cdots, W_j^{n_r}\right]^T$$

$$W_j^r = \frac{\mu_{A_j^r}\left(s_j\right)}{\sum_{r=1}^{n_r} \mu_{A_j^r}\left(s_j\right)} \tag{31}$$

Consider the following fuzzy sliding mode control (FSMC) with m inputs as $s_1, \cdots, s_m$ and n outputs as $\tau_1^{fuzz}, \cdots, \tau_n^{fuzz}$:

$$\tau^{fuzz} = \left[\tau_1^{fuzz}\left(s_1 \mid \theta_1\right), \cdots, \tau_n^{fuzz}\left(s_m \mid \theta_n\right)\right]^T \tag{32}$$

If the mathematical modeling of the system is exact, the output of the controller is denoted by:

$$\tau^{*fuzz} = \left[\tau_1^{*fuzz}\left(s_1 \mid \theta_1^*\right), \cdots, \tau_n^{*fuzz}\left(s_n \mid \theta_n^*\right)\right]^T \tag{33}$$

The approximation of the equivalent control by a fuzzy system is not exact, then:

$$\tau_j^{eq} = \tau_j^{*fuzz}\left(s_j \mid \theta_j^*\right) + \delta_j, \ |\delta_j| < e_j \tag{34}$$

where δ_j is the approximation error which is assumed to be bounded by e_j. Furthermore, θ^* is a matrix which stacks the vectors of optimal values of θ_j:

$$\theta^* = \left[\theta_1^*, \cdots, \theta_n^*\right]^T, \ \theta_j^* \triangleq \arg\min_{\theta_j}\{|\theta_j^T W_j - \tau_j^{eq}|\} \tag{35}$$

11

The most parameters of the previous equations such as uncertainties or error bounds and the optimal values of θ_j cannot be simply determined in advance. Accordingly, they should be estimated. Representing the estimation of e_j by $\hat{e}_j$, the estimation error is:

$$\tilde{e}_j(t) = e_j - \hat{e}_j(t) \tag{36}$$

Therefore, the equivalent part of input, τ^{eq}, can be estimated by the fuzzy system as:

$$\hat{\tau} = \left[\hat{\tau}_1 \left(s_1 \mid \hat{\theta}_1 \right), \cdots, \hat{\tau}_n \left(s_n \mid \hat{\theta}_n \right) \right]^T$$
$$\hat{\tau}_j \left(s_j \mid \hat{\theta}_j \right) = \hat{\theta}_j^T W_j, \, j = 1, \cdots, n \tag{37}$$

in which $\hat{\theta}_j$ is the estimated value of θ_j^*. In this case, the control law is considered as follows:

$$\tau_j = - \left(\hat{\tau}_j \left(s_j \mid \hat{\theta}_j \right) + \hat{\tau}_j^{rb} \left(s_j \right) \right) \tag{38}$$

By substituting Eq. (38) into Eq. (19) and using Eq. (21), we have:

$$M\dot{s} + Cs = -\hat{\tau} \left(s \mid \hat{\theta} \right) - \hat{\tau}^{rb}(s) + \tau^{eq} \tag{39}$$

Let define:

$$\tilde{\tau} = \tau^{eq} - \hat{\tau} \left(s \mid \hat{\theta} \right) \tag{40}$$

Putting Eq. (34) into above equation gives:

$$\begin{aligned} \tilde{\tau} &= \tau^{*fuzz} \left(s \mid \theta^* \right) - \hat{\tau} \left(s \mid \hat{\theta} \right) + \Delta \\ &= \theta^{*T} W - \hat{\theta}^T W + \Delta = \left(\theta^* - \hat{\theta} \right)^T W + \Delta \\ &= \tilde{\theta}^T W + \Delta, \, \tilde{\theta} = \theta^* - \hat{\theta} \end{aligned} \tag{41}$$

where $\Delta = [\delta_1, \cdots, \delta_n]^T$.

Theorem 1. *Consider Eq. (1) as the dynamic equations of a manipulator contacting the environment. Suppose that the control torque is:*

$$\tau = - \left(\hat{\tau} \left(s \mid \hat{\theta} \right) + \hat{\tau}^{rb} \left(s \mid \hat{\alpha} \right) \right) \tag{42}$$

where $\hat{\tau} \left(s \mid \hat{\theta} \right)$ is given in Eq. (37) and $\hat{\tau}^{rb}$ is:

$$\hat{\tau}^{rb} = \left[\hat{\tau}_1^{rb} \left(s_1 \mid \hat{\alpha}_1 \right), \cdots, \hat{\tau}_n^{rb} \left(s_n \mid \hat{\alpha}_n \right) \right]^T$$
$$\hat{\tau}_j^{rb} \left(s_j \mid \hat{\alpha}_j \right) = \hat{\alpha}_j^T \zeta_j \left(s_j \right) \tag{43}$$

12

where $\zeta_j\left(s_j\right) = \left[s_j, \int s_j dt\right]^T$ and $\alpha_j = \left[K_{Pj}, K_{Ij}\right]^T$. *Also, the adaptation laws are expressed by:*

$$\dot{\hat{\theta}}_j = \gamma_{j1} s_j W_j$$
$$\dot{\hat{e}}_j = \gamma_{j2}|s_j|$$
$$\dot{\hat{\alpha}}_j = \gamma_{j3} s_j \zeta_j\left(s_j\right) \tag{44}$$

where $\gamma_{j1}, \gamma_{j2}, \gamma_{j3}$ are positive constants. Then, the sliding surface defined in (16) converges to zero, asymptotically.

PROOF. Let define $z_j = \left[s_j, \tilde{e}_j, \tilde{\theta}_j, \tilde{\alpha}_j\right]^T$, $Z = [z_1, z_2, \cdots, z_n]^T$ and Lyapunov candidate function as:

$$V(Z) = \frac{1}{2}s^T M s + \frac{1}{2}\sum_{j=1}^{n}\left(\frac{\tilde{\theta}_j^T \tilde{\theta}_j}{\gamma_{j1}} + \frac{\tilde{e}_j^2}{\gamma_{j2}} + \frac{\tilde{\alpha}_j^T \tilde{\alpha}_j}{\gamma_{j3}}\right) \tag{45}$$

Differentiating the above equation with respect to time yields:

$$\dot{V}(Z) = s^T M \dot{s} + \frac{1}{2}s^T \dot{M} s + \sum_{j=1}^{n}\left(\frac{\tilde{\theta}_j^T \dot{\tilde{\theta}}_j}{\gamma_{j1}} + \frac{\tilde{e}_j \dot{\tilde{e}}_j}{\gamma_{j2}} + \frac{\tilde{\alpha}_j^T \dot{\tilde{\alpha}}_j}{\gamma_{j3}}\right) \tag{46}$$

in which $\tilde{\alpha}_j = \alpha_j^* - \hat{\alpha}_j$. $\tilde{e}$ and $\tilde{\theta}$ are defined in Eqs. (36) and (41), respectively.

$$\begin{aligned}
\dot{V}(Z) &= s^T\left(M\dot{s} + Cs\right) - \sum_{j=1}^{n}\left(\frac{\tilde{\theta}_j^T \dot{\tilde{\theta}}_j}{\gamma_{j1}} + \frac{\tilde{e}_j \dot{\tilde{e}}_j}{\gamma_{j2}} + \frac{\tilde{\alpha}_j^T \dot{\hat{\alpha}}_j}{\gamma_{j3}}\right) \\
&= \sum_{j=1}^{n}\left(\tilde{\theta}_j^T s_j W_j + s_j \delta_j - s_j \hat{\tau}_j^{rb}\left(s_j\right) - \frac{\tilde{\theta}_j^T \dot{\hat{\theta}}_j}{\gamma_{j1}}\right. \\
&\quad \left. -\frac{\tilde{e}_j \dot{\hat{e}}_j}{\gamma_{j2}} - \frac{\tilde{\alpha}_j^T \dot{\hat{\alpha}}_j}{\gamma_{j3}}\right) = \sum_{j=1}^{n}\left(\tilde{\theta}_j^T\left(s_j W_j - \frac{\dot{\hat{\theta}}_j}{\gamma_{j1}}\right)\right. \\
&\quad \left. +s_j \delta_j - s_j\left(\tau_j^{*rb} - \tilde{\alpha}_j^T \zeta_j\right) - \frac{\tilde{e}_j \dot{\hat{e}}_j}{\gamma_{j2}} - \frac{\tilde{\alpha}_j^T \dot{\hat{\alpha}}_j}{\gamma_{j3}}\right) \\
&= \sum_{j=1}^{n}\left(\tilde{\theta}_j^T\left(s_j W_j - \frac{\dot{\hat{\theta}}_j}{\gamma_{j1}}\right) + \tilde{\alpha}_j^T\left(s_j \zeta_j - \frac{\dot{\hat{\alpha}}}{\gamma_{j3}}\right)\right. \\
&\quad \left. +\left[s_j\left(\delta_j - \tau_j^{*rb}\right) - \frac{\tilde{e}_j \dot{\hat{e}}_j}{\gamma_{j2}}\right]\right) \tag{47}
\end{aligned}$$

13

By applying the adaptation laws in 44, it is obtained:

$$\dot{V}(Z) = \sum_{j=1}^{n} \left[s_j \left(\delta_j - \tau_j^{*rb} \right) - \tilde{e}_j |s_j| \right]$$

$$= \sum_{j=1}^{n} \left[s_j \left(\delta_j - \tau_j^{*rb} \right) - e_j |s_j| + \hat{e}_j |s_j| \right]$$

$$\leq \sum_{j=1}^{n} \left[|s_j| \left(|\delta_j| - e_j \right) - s_j \tau_j^{*rb} + \hat{e}_j |s_j| \right] \tag{48}$$

Let define the following approximation error:

$$\vartheta_j = e_j \operatorname{sign}\left(s_j \right) - \tau_j^{*rb} \tag{49}$$

Following the method proposed in [39], the discontinuous control action $e_j \operatorname{sign}\left(s_j \right)$ is approximated by a PI controller inside a boundary layer around the sliding surface to attenuate the chattering problem. However, outside the boundary layer, the robust part of control effort is e_j. Using the above definition, Eq. (48) can be rewritten as:

$$\dot{V}(Z) \leq \sum_{j=1}^{n} \left[|s_j| \left(|\delta_j| - e_j \right) + s_j \vartheta_j \right]$$

$$\leq \sum_{j=1}^{n} \left[|s_j| \left(|\delta_j| - e_j \right) + |s_j| |\vartheta_j| \right]$$

$$= \sum_{j=1}^{n} \left[|s_j| \left(|\delta_j| - e_j + |\vartheta_j| \right) \right] \tag{50}$$

According to the universal approximation theorem, the approximation error, ϑ_j, can become small enough such that based on the assumption expressed in Eq. (34), the following inequality holds:

$$\dot{V}(Z) = \sum_{j=1}^{n} \left[|s_j| \left(|\delta_j| - e_j + |\vartheta_j| \right) \right] \leq 0 \tag{51}$$

which shows that $\dot{V}(Z)$ is negative semidefinite. This verifies the boundedness of $s_j(t)$, $\tilde{e}_j, \tilde{\theta}_j$ and $\tilde{\alpha}_j$. However, conforming to Eq. (16), tracking the defined

14

reference trajectories in force, position, and joint subspaces is ensured when the asymptotic convergence of the sliding surface to zero is shown [38]. Therefore, the following lemma known as Barbalat's lemma [40] is used to guarantee that s_j converges to zero, asymptotically.

Lemma 1. *Let $\phi : R \to R$ be a uniformly continuous function on $[0, \infty)$. Suppose that $lim_{t \to \infty} \int_0^\tau \phi(\tau) d\tau$ exists and finite. Then, $\lim_{t \to \infty} \phi(t) = 0$.*

Now, let define

$$\Gamma_j(t) \triangleq |s_j| \left(e_j - |\delta_j| + |\vartheta_j| \right) \le -\dot{V}(z_j) \tag{52}$$

Integrating both sides of above equation yields:

$$\int_0^t \Gamma_j(r) \, dr \le V(z_j(0)) - V(z_j(t)) \tag{53}$$

where $V(z_j(0)) = V(s_j(0), \tilde{e}_j, \tilde{\theta}_j, \tilde{\alpha}_j)$. Since $V(z_j(0))$ and $V(z_j(t))$ are bounded and also $V(z_j(t))$ is noncreasing, it is deduced that:

$$\lim_{t \to \infty} \int_0^t \Gamma_j(r) \, dr \le \infty \tag{54}$$

According to Barbalat's lemma, Eq. (54) implies $lim_{t \to \infty} \Gamma_j(t) = 0$. From this result and Eq. (52) it is concluded that $lim_{t \to \infty} s_j(t) = 0$. Therefore, it can be also verified that $\tilde{F}$, $K\tilde{x}$ and $J\dot{\tilde{q}}$ converges to zero, asymptotically [38]. The block diagram of the proposed AFSMC method is presented in Fig. 1.

Remark: In accordance with the adaptation laws in Eq. (44), the parameters converge to their desired values in finite time. However, the transient response properties such as settling time and overshoot are affected by different initial values, especially K_{P0} and K_{I0}. Also, the rate of convergence of adaptive parameters is varied by changing γ_j, $j = 1, 2, 3$, and their corresponding initial values. On the other hand, referring to Eq. (13), the value of λ changes the sliding surface, explicitly. Since the sliding surface has a direct and crucial effect on the control input and parameters, it is the most effective variable in control performance. The detailed discussion on how these parameters affect the control performance will be given in the design parameters analysis of the simulation results section.
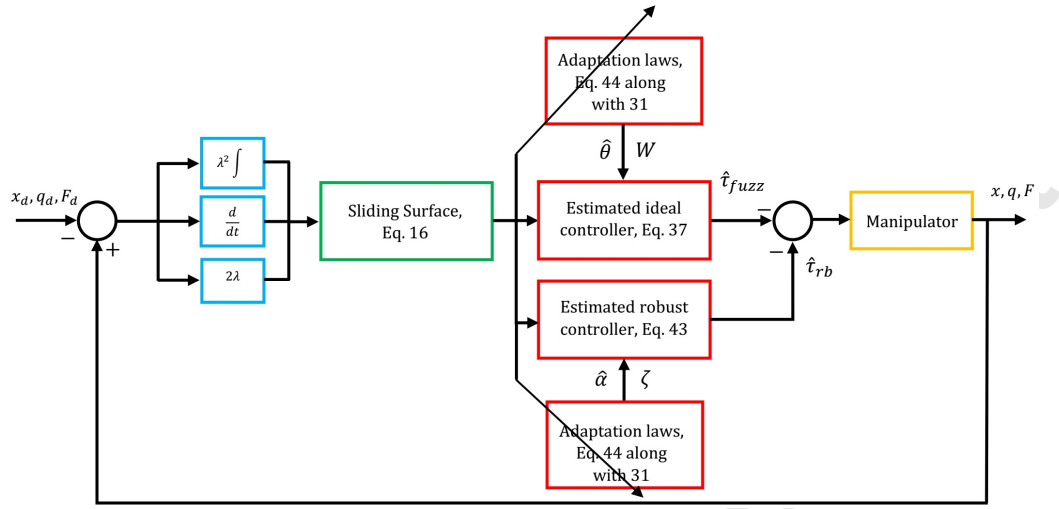
15

Figure 1: Block diagram of proposed AFSMC scheme for hybrid force/position control of manipulators
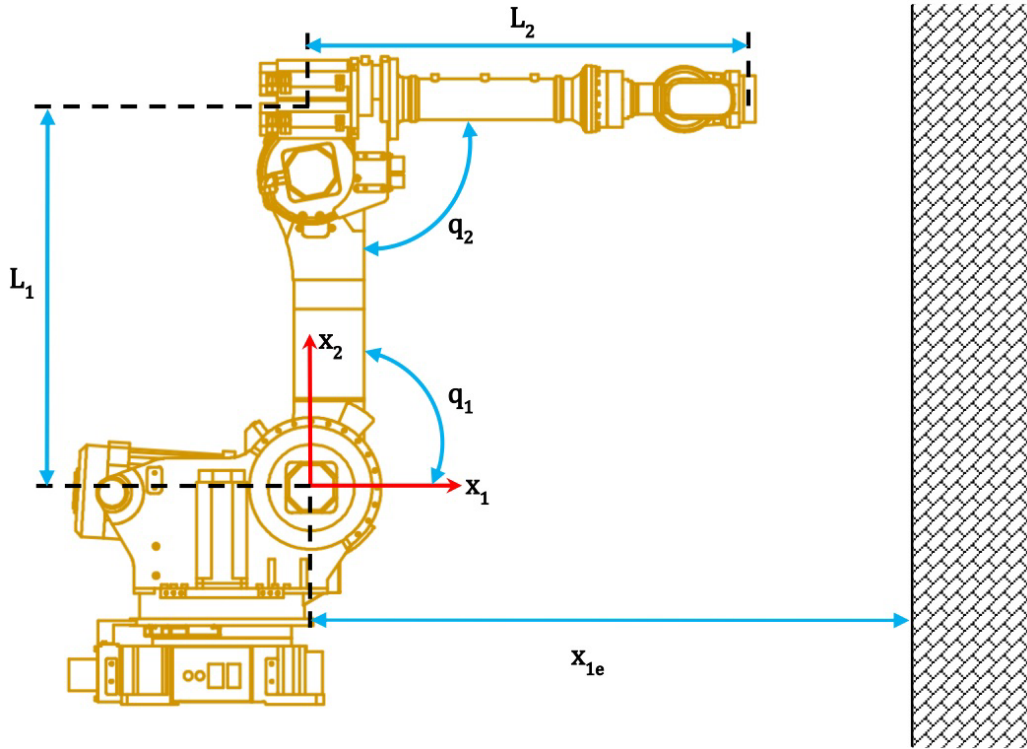

Figure 2: A fixed-base robot manipulator with two-rigid links interacting with a rigid surface [41].

16

Table 1: Numerical values (in SI) of physical and geometrical properties [7]

Parameter	Value
m_1	15.61
m_2	11.36
L_1	0.432
L_2	0.432
k	$1e4$

4. Simulation Results

In order to evaluate the developed controller performance, some simulation studies are carried out on a two-rigid links manipulator interacting with a vertical surface, Fig. 2. The components of M, C and G matrices of Eq. (1) are:

$$M_{11} = m_2 L_2^2 + (m_1 + m_2) L_1^2 + 2L_1 L_2 \cos (q_2)$$
$$M_{12} = m_2 L_2^2 + m_2 L_1 L_2 \cos (q_2), \; M_{21} = M_{12}$$
$$M_{22} = m_2 L_2^2$$
$$C_{11} = -m_2 L_1 L_2 \dot{q}_2 \sin (q_2)$$
$$C_{12} = -m_2 L_1 L_2 (\dot{q}_1 + \dot{q}_2) \sin (q_2)$$
$$C_{21} = m_2 L_1 L_2 \dot{q}_1 \sin (q_2) , \; C_{22} = 0$$
$$G_1 = (m_1 + m_2) L_1 g \cos (q_1) + m_2 L_2 g \cos (q_2)$$
$$G_2 = m_2 L_2 g \cos (q_1 + q_2) \tag{55}$$

The physical and geometrical properties of the robot and environment are summarized in Table 1. The goal is to control the force and position in the x_1 and x_2-directions, respectively. The desired trajectories for force and position are considered as: $F_d = 20 \, N$ and $x_{2d} = 0.5 (1 - \exp (-t))$. Also, it can be confirmed that $K^+ = 1/k$, $K^- = [0 \, 0; 0 \, 1]$, $J^+ = J^{-1}$ and $J^- = 0$ [7]. The distance from the origin of the inertial reference frame to the surface along x_1-axis is considered as $x_{1e} = 0.61 \, m$. Therefore, the interaction force between the end-effector and the environment developed during operation is $F = k (x_1 - x_{1e})$. Also, the initial values for design parameters are given in Table 2 which have been selected by iterations and following the results.

The set of MFs for both s_1 and s_2 are identical and illustrated in Fig. 3 where the figure's legend stands for N:negative, B:big, M:medium, S:small, P:positive. These MFs have been selected as follows: By changing λ while keeping the other

17

Table 2: Considered numerical values for design parameters of the controller

Parameter	Value
γ_{j1}	1
γ_{j2}	1
γ_{j3}	1
λ	1
K_{P0}	1000
K_{I0}	10000
$\hat{E}_0$	0.5
$\hat{\theta}_0^T$	$[-7.5 \; -5 \; -2.5 \; 0 \; 2.5 \; 5]$

design parameters unchanged, the range of variations of sliding surface is obtained and divided into several equal intervals. Then, the considered MFs are distributed symmetrically with respect to the range of variations of sliding surface. It is worth noting that the number of MFs and their mean and variance have been selected by trial and error. The mathematical equations of MFs are:

$$\mu_{NB}\left(s_j\right) = \frac{1}{1 + \exp\left(\frac{s_j + 0.2}{50}\right)}$$

$$\mu_{NM}\left(s_j\right) = \exp\left(\frac{-\left(s_j + 0.12\right)^2}{0.0008}\right)$$

$$\mu_{NS}\left(s_j\right) = \exp\left(\frac{-\left(s_j + 0.04\right)^2}{0.0008}\right)$$

$$\mu_{PS}\left(s_j\right) = \exp\left(\frac{-\left(s_j - 0.04\right)^2}{0.0008}\right)$$

$$\mu_{PM}\left(s_j\right) = \exp\left(\frac{-\left(s_j - 0.12\right)^2}{0.0008}\right)$$

$$\mu_{PB}\left(s_j\right) = \frac{1}{1 + \exp\left(\frac{s_j - 0.2}{-50}\right)} \tag{56}$$

18
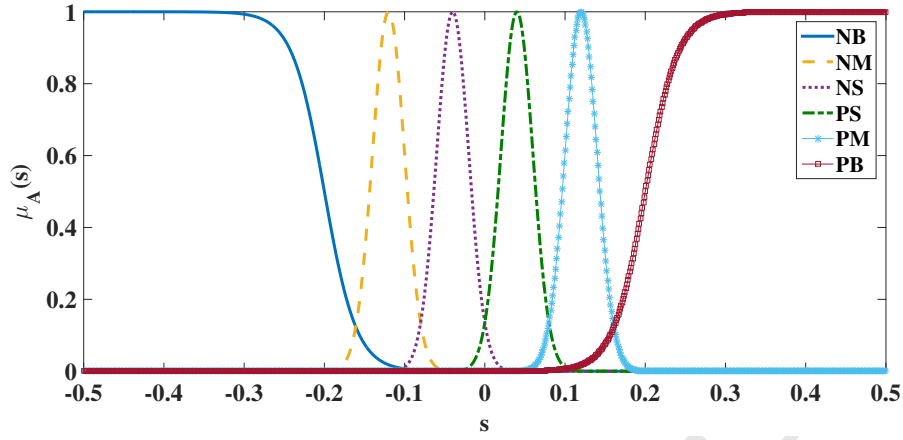
Figure 3: The set of Gaussian MFs for fuzzification of the sliding surfaces, s_1 and s_2

According to Theorem 1, s_j is the most important element in controller design. Referring to Eq. (16), it is clear that all the required data about the plant model and environment is J and K. To construct the J matrix, the length of the manipulator links should be determined in advance. Thus, the control input can be implemented by just having an estimation of the length of the links and stiffness coefficient of the environment.

4.1. Performance Results

The controller performance is initially investigated for the case that the exact values of L_j, $j = 1, 2$, and k are known. The results of this study are provided in Fig. 4. It is shown in Fig. 4b that the controlled system tracks the desired trajectory in the x_2-direction in a few seconds. Also, Figs. 4a and 4c depict the system response in the face of constrained direction, x_1. It can be seen that the system output is desirable for both transient and steady-state responses. It should be noted that this performance is achieved despite the lack of information about the system dynamic model.

The joint trajectories of the robotic arm and their input torques are plotted in Fig. 5. This figure clarifies that the joints converge to their final values by the bounded and chattering-free control inputs.

For the second case, it is assumed that the stiffness coefficient of the environment and the length of manipulator links are not known and their estimations are used in the controller. The effect of imprecise knowledge about the stiffness coefficient on the system performance is drawn in Fig. 6. As indicated in Figs. 6a
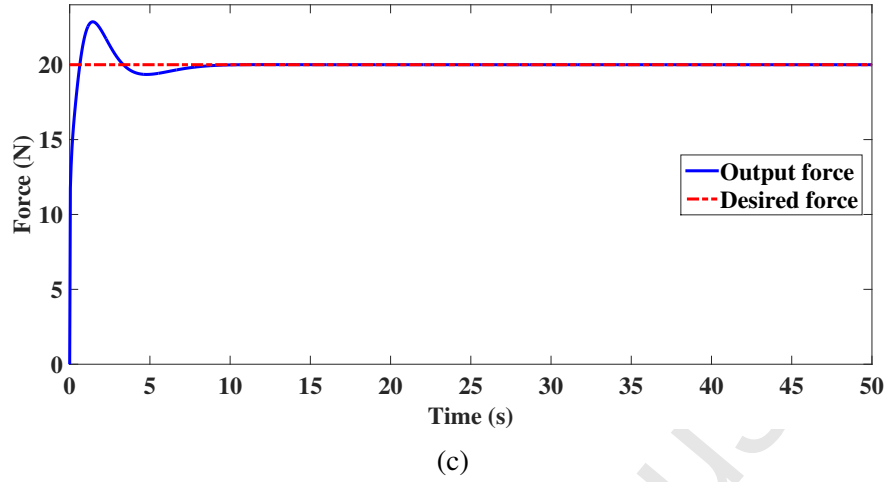
19

(a)

(b)

Figure 4: a-b

20

(c)
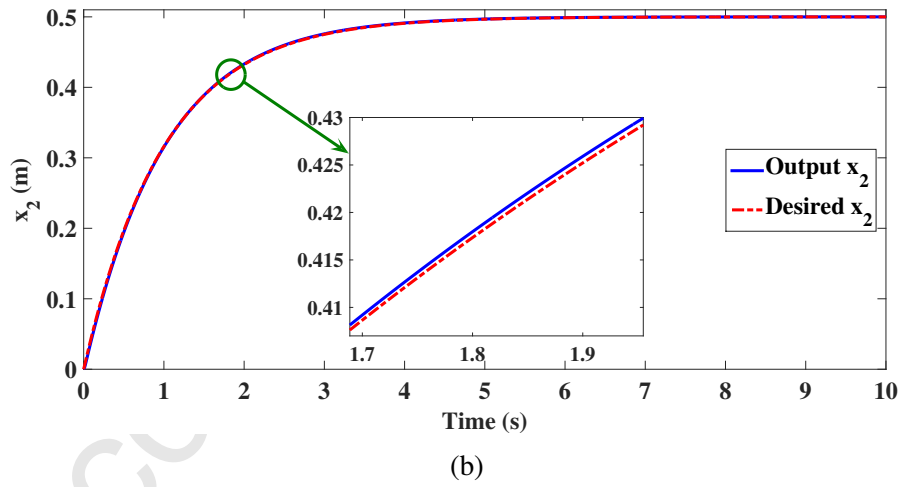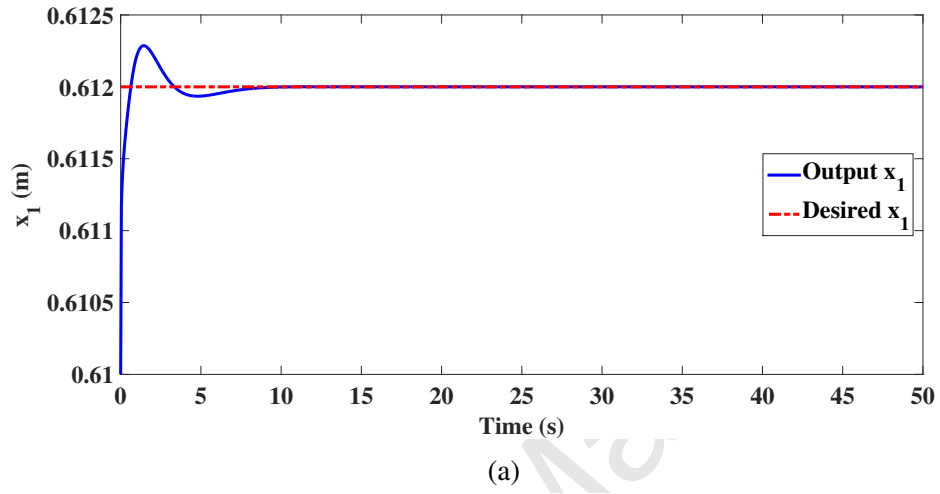
Figure 4: System trajectory tracking by the proposed AFSMC when the plant model is known, a) x_1-direction, b) x_2-direction c) Applied force along x_1-axis

and 6c, increasing the estimated coefficient causes an increase in properties such as overshoot and settling time in tracking the desired reference force trajectory. However, lack of information about k has an insignificant effect on tracking the desired position trajectory along x_2-axis, and the trajectories overlap the reference one, quickly.

Fig. 7 demonstrates the effects of inaccurate information about the length of manipulator links on the controller performance. Considering Figs. 7a and 7c, as the estimated L increases, the overshoot increases, slightly. However, the differences between settling times are not considerable. In addition, Fig. 7b reveals that the system converges to the desired trajectory in the x_2-direction in a few seconds.

In Fig. 8, the uncertainties about k and L are taken into consideration, simultaneously. Comparing Fig. 8 with Figs. 6 and 7, it is observed that the overshoot and settling time are increased more than considering uncertainty about k and L, separately. Also, as it can be deduced from Fig. 8b, the position response of the system along x_2-axis is still less affected by the uncertainties.

From the discussion above, it is concluded that the inaccurate estimation of the stiffness coefficient has more adverse effects on the controlled system performance than the length of manipulator links. Moreover, the force response of the system is more influenced by uncertainties than the position response. However, in all cases, the controller performance is satisfactory without the requirement to have
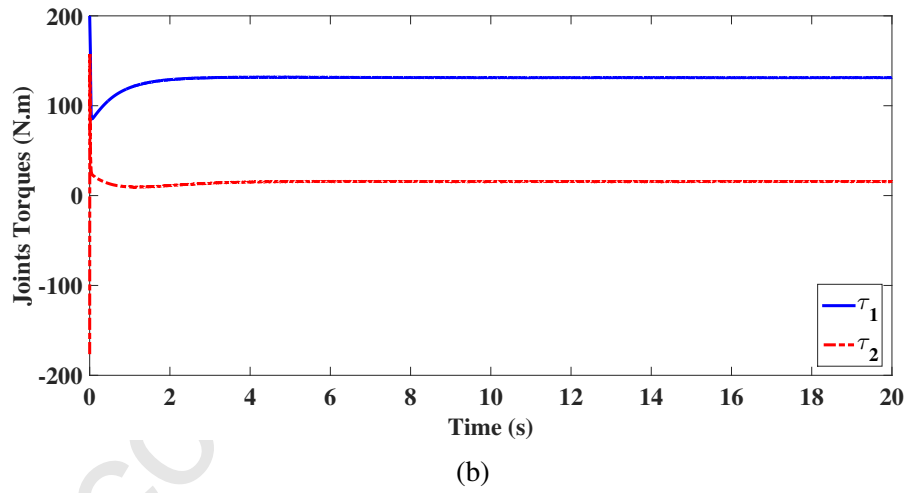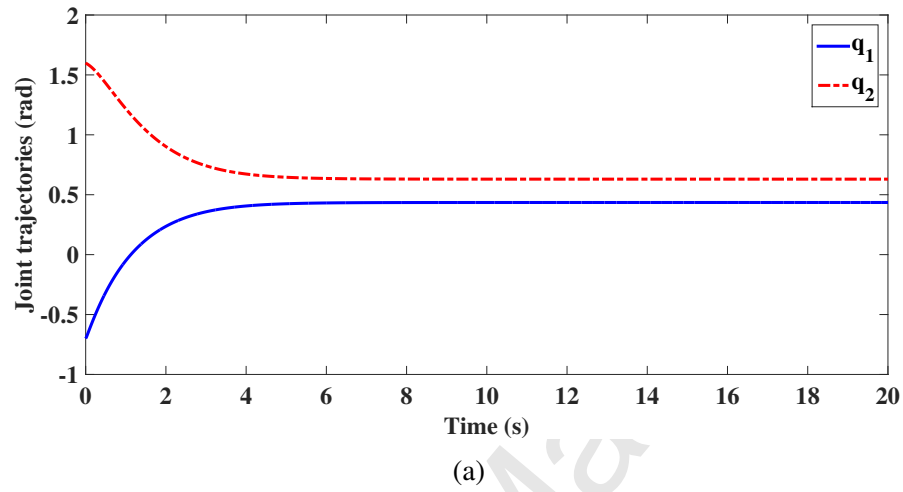
21

(a)

(b)

Figure 5: a) Joint trajectories, b) Generated control inputs by applying the proposed AFSMC on the simulation case study when the plant model is known.
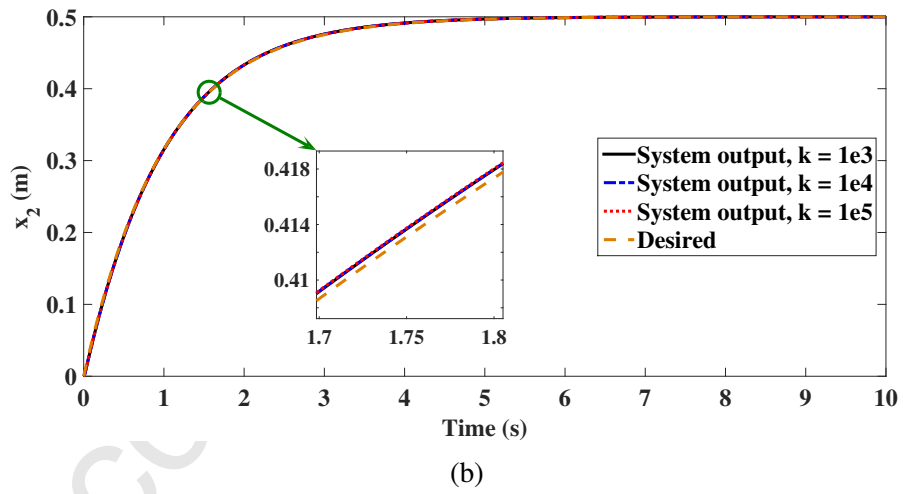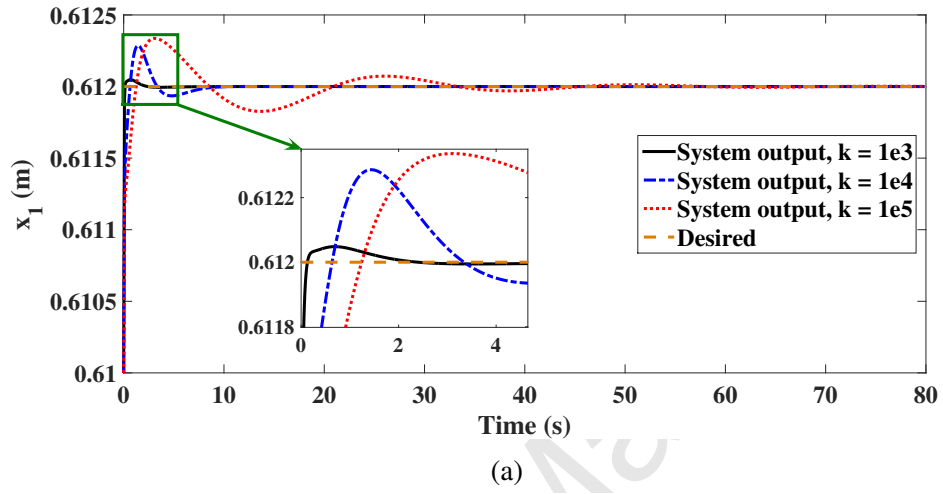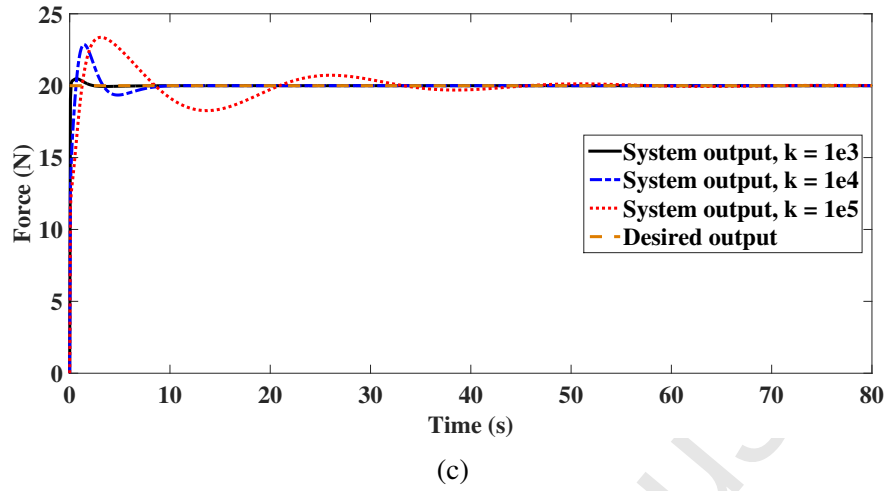
22

(a)

(b)

Figure 6: a-b

23

(c)

Figure 6: Effects of imprecise knowledge about the stiffness coefficient of the environment on the controlled system for a) x_1-direction, b) x_2-direction and c) Applied force along x_1-axis

an estimation of dynamic model structure and properties such as the masses.

4.2. Design Parameters Analysis

As mentioned previously, although the PI controller gains converge to their true values in finite time according to Eq. (44), their different initial values affect the controller performance. Table 3 lists the various initial values for PI controller gains and their effects on some important variables. As indicated in this table, increasing K_{I0} causes a further decrease in applied force along x_2-axis than that of K_{P0}. Also, by increasing K_{I0}, the required torques for performing the operation increase much lower than that of K_{P0}.

On the other hand, since the most important element of the controller is s_j, changing λ has more notable effects on the system output than the others. The effect of changing λ on the output force trajectory is shown in Fig. 9 where λ is varied from 0.1 to 2. It is evident that increasing λ leads to an increase in the overshoot and a decreases in the settling time. However, the higher overshoot with larger λ means a larger applied force which can be destructive for both the environment and end-effector. For the values larger than $\lambda = 2$ this trend continues until the system becomes unstable for λ about 4.
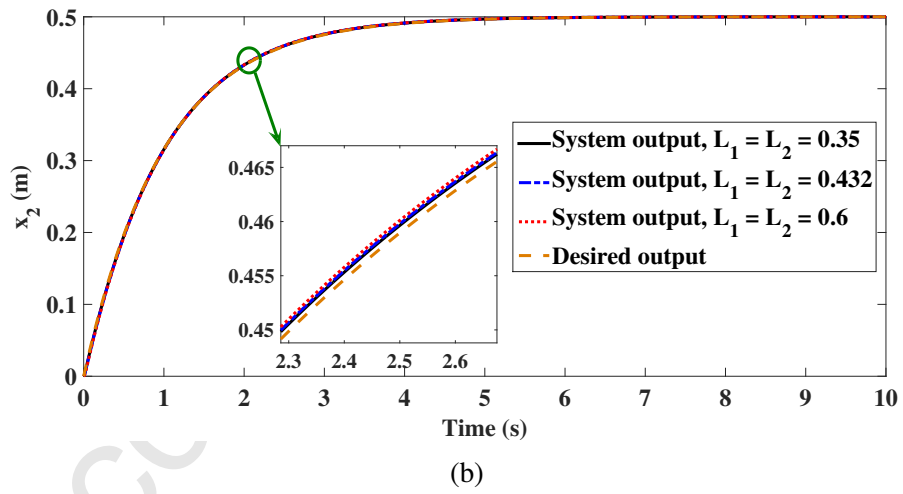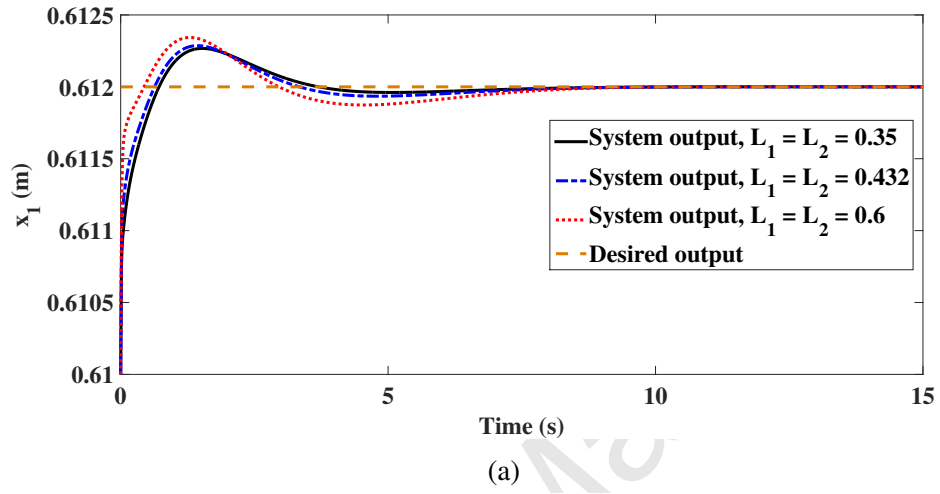
24

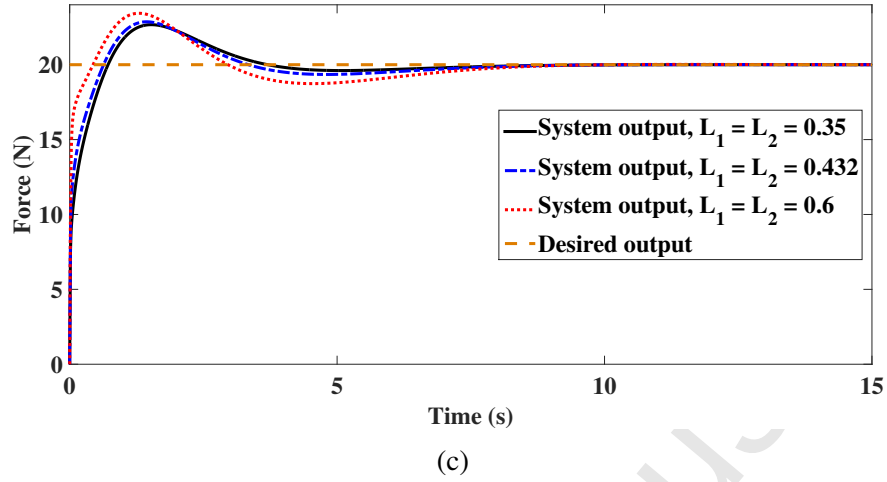(a)

(b)

Figure 7: a-b

25

(c)

Figure 7: Effects of imprecise knowledge about the length of the manipulator links on the controlled system for a) x_1-direction, b) x_2-direction and c) Applied force along x_1-axis

4.3. Comparative Results

The performance of the proposed AFSMC controller in desired force trajectory tracking and its error are compared with two SMC controllers in Figs.10a and 10b, respectively. SMC1 is a sliding mode-based controller in which the robust part of the controller contains the sign function while this function is replaced with a sigmoid type function in SMC2 to reduce chattering. Being completely model-free is the main advantage of the proposed AFSMC controller, in the current work, in comparison with the robust model-based controllers such as SMC1 and SMC2. However, in this section, the system parameters are supposed to be almost known and the performance of the controllers are compared in coping with uncertainties. It is shown in Fig.10a that the system responses in the transient phase are almost identical for all controllers and they can achieve their final desired values in a very short time. Nevertheless, the superiority of the presented AFSMC is clear in the steady-state part of the response as shown in the enlarged sections of the figure.

5. Conclusion and Future Work

In this study, an extended AFSMC scheme for hybrid force/position control of robotic arms interacting with totally unknown rigid surfaces is presented. Being independent of plant mathematical model and physical properties of environment is the most important advantage of the presented method compared with those
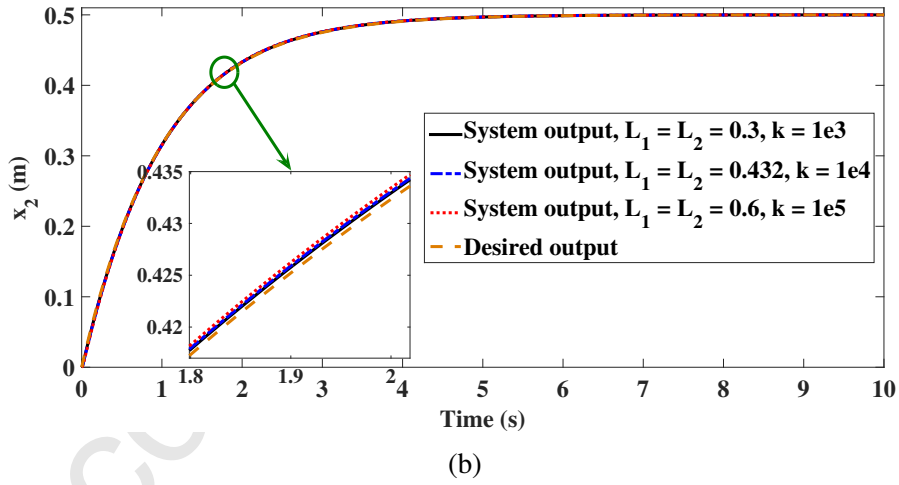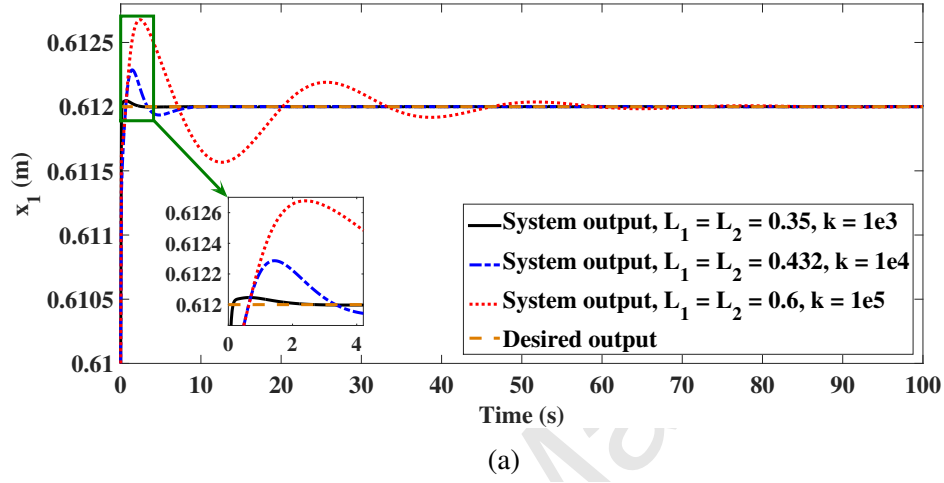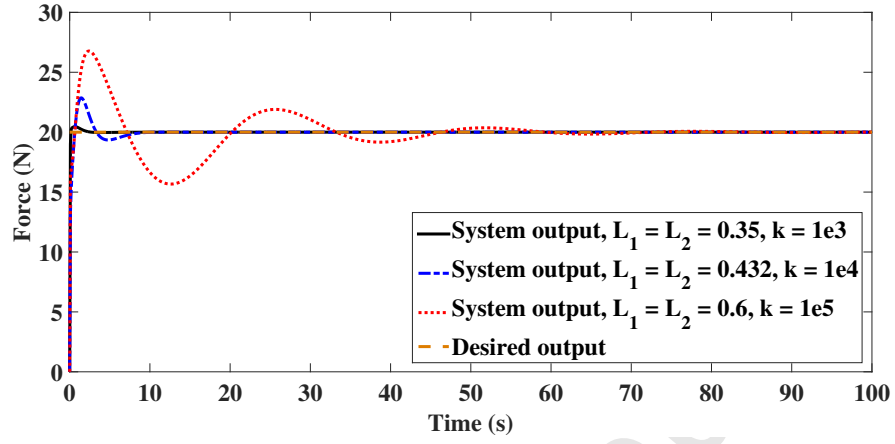
26

(a)

(b)

Figure 8: a-b

27

(c)

Figure 8: Effects of imprecise knowledge about the length of manipulator links and stiffness coefficient of the environment on the controlled system for a) x_1-direction, b) x_2-direction and c) Applied force along x_1-axis
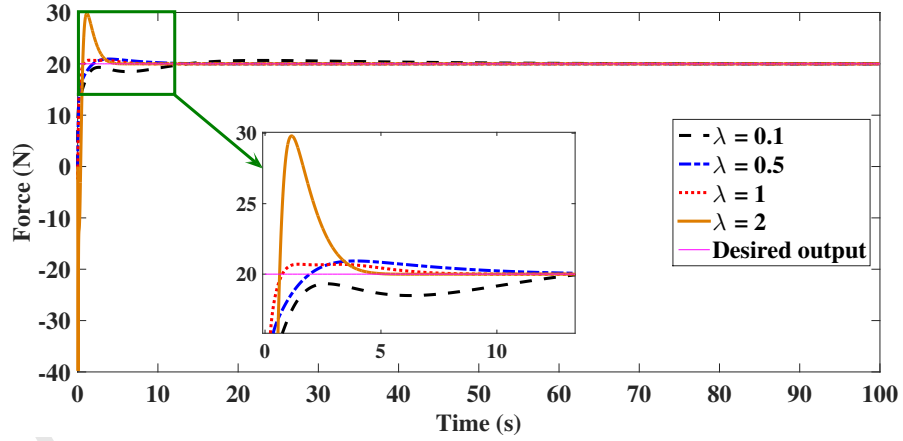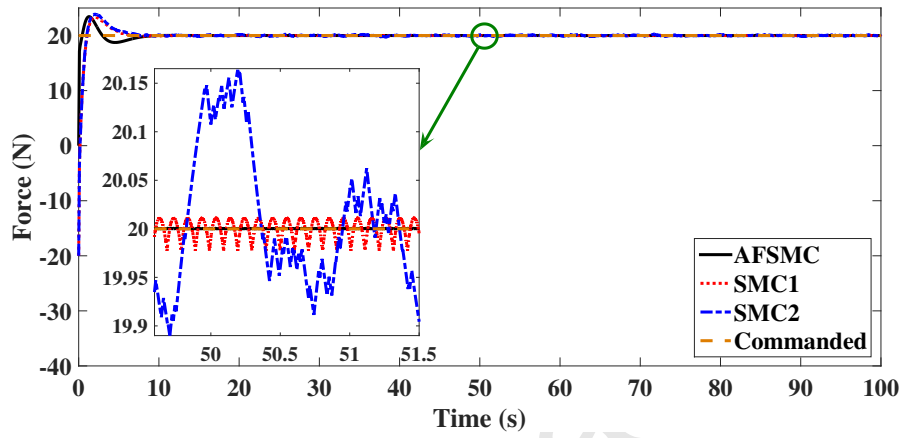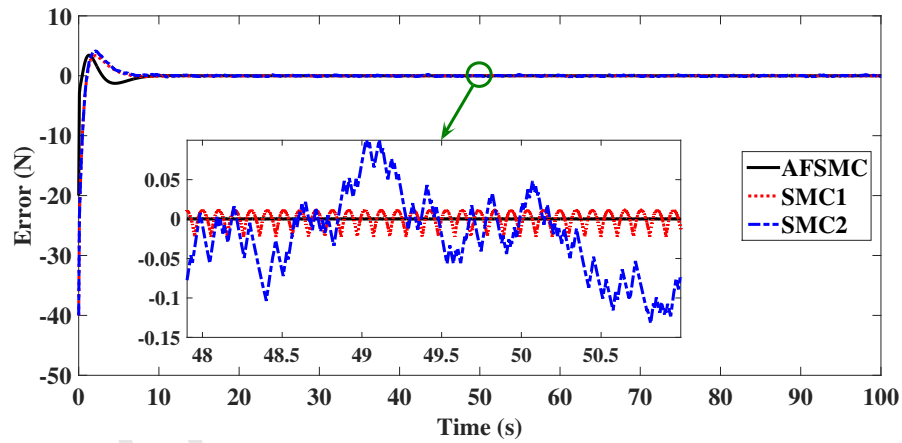

Figure 9: Effects of changing λ on the controller performance in force trajectory tracking

28

(a)

(b)

Figure 10: Performance comparison of proposed AFSMC with SMC1 and SMC2 in coping with uncertainties, a) Force trajectory tracking and b) Error in force trajectory tracking

29

Table 3: Initial values for PI controller gains

Initial gains	$\max(x_1)$	$\max(F)$	$\max(|\tau_1|)$	$\max(|\tau_2|)$
$K_{P0} = 100$ $K_{I0} = 100$	0.6221	121.2892	149.8136	27.9641
$K_{P0} = 150$ $K_{I0} = 100$	0.6221	120.5161	149.4271	34.7235
$K_{P0} = 100$ $K_{I0} = 150$	0.6213	112.7963	148.2077	28.1165
$K_{P0} = 150$ $K_{I0} = 150$	0.6213	112.7133	148.0053	34.9203
$K_{P0} = 300$ $K_{I0} = 150$	0.6207	107.3273	281.3320	56.0344
$K_{P0} = 150$ $K_{I0} = 300$	0.6193	92.9236	145.1045	35.5135
$K_{P0} = 300$ $K_{I0} = 300$	0.6192	91.6388	281.3320	56.3469
$K_{P0} = 450$ $K_{I0} = 300$	0.6187	86.6108	418.2479	76.9534
$K_{P0} = 300$ $K_{I0} = 450$	0.6180	80.0001	281.3320	56.6598
$K_{P0} = 100$ $K_{I0} = 450$	0.6189	89.1374	142.7592	30.0929

published up to now. Besides that, the requirement for determinig the bounds of uncertainties is removed by this method. For this purpose, the dynamic model structure is decomposed into position, force, and redundant joint subspaces. The equivalent part of the controller which is constructed based on SMC concept is approximated by TSK fuzzy system and the robust part is estimated by an adaptive PI controller. The simulation results indicate that the synthesized controller has a satisfactory performance in dealing with uncertainties. Also, the superiority of the current AFSMC method in relation to classical model-based methods such as SMC is confirmed.

For future study, the presented AFSMC method can be extended to full-actuated or under-actuated mobile manipulators. In addition, the proposed method in the current study is restricted to force control problems in which the position, force, and redundant joint subspaces are orthogonal to each other. The generalization of

30

the presented method to other force control schemes such as impedance control is also a future direction.

31

References

[1] B. Siciliano, O. Khatib, Springer handbook of robotics, Springer, 2016.

[2] F. L. Lewis, D. M. Dawson, C. T. Abdallah, Robot manipulator control: theory and practice, CRC Press, 2003.

[3] J. Yu, Y. Ma, H. Yu, C. Lin, Reduced-order observer-based adaptive fuzzy tracking control for chaotic permanent magnet synchronous motors, Neurocomputing 214 (2016) 201–209.

[4] J. Lian, J. Hu, S. H. Żak, Variable neural adaptive robust control: A switched system approach, IEEE transactions on neural networks and learning systems 26 (5) (2015) 903–915.

[5] T. Wang, J. Qiu, S. Yin, H. Gao, J. Fan, T. Chai, Performance-based adaptive fuzzy tracking control for networked industrial processes, IEEE transactions on cybernetics 46 (8) (2016) 1760–1770.

[6] P. Shi, Sliding-mode control for fractional-order nonlinear systems based on disturbance observer, Robust Adaptive Control for Fractional-Order Systems with Disturbance and Saturation (2018) 85–94.

[7] C. Kwan, Hybrid force/position control for manipulators with motor dynamics using a sliding-adaptive approach, IEEE Transactions on Automatic Control 40 (5) (1995) 963–968.

[8] M. Farooq, D. B. Wang, N. Dar, Adaptive sliding-mode hybrid force/position controller for flexible joint robot, in: Mechatronics and Automation, 2008. ICMA 2008. IEEE International Conference on, IEEE, 2008, pp. 724–731.

[9] C.-C. Cheah, Y. Zhao, J.-J. E. Slotine, Adaptive Jacobian motion and force tracking control for constrained robots with uncertainties, in: Robotics and Automation, 2006. ICRA 2006. Proceedings 2006 IEEE International Conference on, IEEE, 2006, pp. 2226–2231.

[10] R. Mohajerpoor, M. Rezaei, A. Talebi, M. Noorhosseini, R. Monfaredi, A robust adaptive hybrid force/position control scheme of two planar manipulators handling an unknown object interacting with an environment, Proceedings of the Institution of Mechanical Engineers, Part I: Journal of Systems and Control Engineering 226 (4) (2012) 509–522.

32

[11] J. Fei, C. Lu, Adaptive sliding mode control of dynamic systems using double loop recurrent neural network structure, IEEE transactions on neural networks and learning systems.

[12] Y. Chu, J. Fei, S. Hou, Dynamic global proportional integral derivative sliding mode control using radial basis function neural compensator for three-phase active power filter, Transactions of the Institute of Measurement and Control (2017) 0142331217726955.

[13] J. Fei, C. Lu, Adaptive fractional order sliding mode controller with neural estimator, Journal of the Franklin Institute.

[14] L. Chen, M. Liu, X. Huang, S. Fu, J. Qiu, Adaptive fuzzy sliding mode control for network-based nonlinear systems with actuator failures, IEEE Transactions on Fuzzy Systems.

[15] J. Zhang, P. Shi, Y. Xia, Robust adaptive sliding-mode control for fuzzy systems with mismatched uncertainties, IEEE Transactions on Fuzzy Systems 18 (4) (2010) 700–711.

[16] A. Poursamad, A. H. Davaie-Markazi, Robust adaptive fuzzy control of unknown chaotic systems, Applied Soft Computing 9 (3) (2009) 970–976.

[17] A. Poursamad, A. H. Markazi, Adaptive fuzzy sliding-mode control for multi-input multi-output chaotic systems, Chaos, Solitons & Fractals 42 (5) (2009) 3100–3109.

[18] R.-E. Precup, H. Hellendoorn, A survey on industrial applications of fuzzy control, Computers in Industry 62 (3) (2011) 213–226.

[19] C.-M. Lin, C.-F. Hsu, Adaptive fuzzy sliding-mode control for induction servomotor systems, IEEE Transactions on Energy Conversion 19 (2) (2004) 362–368.

[20] A. Saghafinia, H. W. Ping, M. N. Uddin, K. S. Gaeid, Adaptive fuzzy sliding-mode control into chattering-free IM drive, IEEE Transactions on Industry Applications 51 (1) (2015) 692–701.

[21] C.-L. Hwang, C.-Y. Kuo, A stable adaptive fuzzy sliding-mode control for affine nonlinear systems with application to four-bar linkage systems, IEEE Transactions on Fuzzy Systems 9 (2) (2001) 238–252.

33

[22] A. Mousavi, A. H. Davaie-Markazi, S. Masoudi, Comparison of adaptive fuzzy sliding-mode pulse width modulation control with common model-based nonlinear controllers for slip control in antilock braking systems, Journal of Dynamic Systems, Measurement, and Control 140 (1) (2018) 011014.

[23] Y. Guo, P.-Y. Woo, An adaptive fuzzy sliding mode controller for robotic manipulators, IEEE Transactions on Systems, Man, and Cybernetics-Part A: Systems and Humans 33 (2) (2003) 149–159.

[24] A. F. Amer, E. A. Sallam, W. M. Elawady, Adaptive fuzzy sliding mode control using supervisory fuzzy control for 3 DOF planar robot manipulators, Applied Soft Computing 11 (8) (2011) 4943–4953.

[25] H. Li, J. Yu, C. Hilton, H. Liu, Adaptive sliding-mode control for nonlinear active suspension vehicle systems using T–S fuzzy approach, IEEE Transactions on Industrial Electronics 60 (8) (2013) 3328–3338.

[26] S. Barghandan, M. A. Badamchizadeh, M. R. Jahed-Motlagh, Improved adaptive fuzzy sliding mode controller for robust fault tolerant of a quadrotor, International Journal of Control, Automation and Systems 15 (1) (2017) 427–441.

[27] N. Kumar, V. Panwar, N. Sukavanam, S. P. Sharma, J.-H. Borm, Neural network based hybrid force/position control for robot manipulators, International Journal of Precision Engineering and Manufacturing 12 (3) (2011) 419–426.

[28] J. Lin, C. Lin, H.-S. Lo, Hybrid position/force control of robot manipulators mounted on oscillatory bases using adaptive fuzzy control, in: Intelligent Control (ISIC), 2010 IEEE International Symposium on, IEEE, 2010, pp. 487–492.

[29] F.-Y. Hsu, L.-C. Fu, Intelligent robot deburring using adaptive fuzzy hybrid position/force control, IEEE Transactions on Robotics and Automation 16 (4) (2000) 325–335.

[30] H. Chaudhary, V. Panwar, R. Prasad, N. Sukavanam, Adaptive neuro fuzzy based hybrid force/position control for an industrial robot manipulator, Journal of Intelligent Manufacturing 27 (6) (2016) 1299–1308.

34

[31] K. Kiguchi, T. Fukuda, Position/force control of robot manipulators for geometrically unknown objects using fuzzy neural networks, IEEE Transactions on Industrial Electronics 47 (3) (2000) 641–649.

[32] N. Mendes, P. Neto, Indirect adaptive fuzzy control for industrial robots: a solution for contact applications, Expert Systems with Applications 42 (22) (2015) 8929–8935.

[33] J. Pliego-Jiménez, M. A. Arteaga-Pérez, Adaptive position/force control for robot manipulators in contact with a rigid surface with uncertain parameters, European Journal of Control 22 (2015) 1–12.

[34] P. Gierlak, M. Szuster, Adaptive position/force control for robot manipulator in contact with a flexible environment, Robotics and Autonomous Systems 95 (2017) 80–101.

[35] A. Jafari, J.-H. Ryu, Independent force and position control for cooperating manipulators handling an unknown object and interacting with an unknown environment, Journal of the Franklin Institute 353 (4) (2016) 857–875.

[36] S. Kilicaslan, M. K. Özgören, S. K. Ider, Hybrid force and motion control of robots with flexible links, Mechanism and Machine Theory 45 (1) (2010) 91–105.

[37] V. Panwar, N. Kumar, N. Sukavanam, J.-H. Borm, Adaptive neural controller for cooperative multiple robot manipulator system manipulating a single rigid object, Applied Soft Computing 12 (1) (2012) 216–227.

[38] R. Lozano, B. Brogliato, Adaptive hybrid force-position control for redundant manipulators, IEEE Transactions on Automatic Control 37 (10) (1992) 1501–1505.

[39] R. Shahnazi, H. M. Shanechi, N. Pariz, Position control of induction and DC servomotors: a novel adaptive fuzzy PI sliding mode control, IEEE Transactions on Energy Conversion 23 (1) (2008) 138–147.

[40] H. K. Khalil, Nonlinear systems, 3rd, New Jewsey, Prentice Hall, 2002.

[41] K. Schulze, Fanuc s-430 robot.
URL https://grabcad.com/library/fanuc-430-robot

35